Journal of Applied Geophysics 145 (2017) 28–38

Contents lists available at ScienceDirect

Journal of Applied Geophysics

journal homepage: www.elsevier.com/locate/jappgeo

The uncertainty of estimating the thickness of soft sediments with the HVSR method: A computational point of view on weak lateral variations

Samuel Bignardi *

University of Ferrara, Department of Physics and Earth Sciences, Via Saragat 1, Office B-216, 40122 Ferrara, Italy
School of Electrical and Computer Engineering, Georgia Institute of Technology, GA, USA

A R T I C L E   I N F O

Article history:
Received 8 March 2017
Received in revised form 3 June 2017
Accepted 26 July 2017
Available online 05 August 2017

Keywords:
Microtremor
HVSR
Bedrock mapping
Lateral variations
Uncertainty

A B S T R A C T

The use of the ratio of microtremor spectra, as computed by the Nakamura's technique, was recently proved successful for the evaluating the thickness of sedimentary covers laying over both shallow and deep rocky bedrocks thus enabling bedrock mapping. The experimental success of such application and its experimental uncertainties are today reported in many publications. To map bedrock, two approaches exist. The first is to assume a constant shear wave velocity profile of the sediments. The second, and most preferable, is Ibs-von Seht and Wohlenberg's, based on correlating Nakamura's curves main peak and wells information. In the latter approach, the main sources of uncertainty addressed by authors, despite the lack of formal proof, comprise local deviations of the subsurface from the assumed model. I first discuss the reliability of the simplified constant velocity approach showing its limitations. As a second task, I evaluate the uncertainty of the Ibs-von Seht and Wohlenberg's approach with focus on local subsurface variations. Since the experimental basis is well established, I entirely focus my investigation on numerical simulations to evaluate to what extent local subsurface deviations from the assumed model may affect the outcome of a bedrock mapping survey. Further, the present investigation strategy suggests that modeling and inversion, through the investigation of the parameters space around the reference model, may reveal a very convenient tool when lateral variations are suspected to exist or when the number of available wells is not sufficient to obtain an accurate frequency-depth regression.

1. Introduction

Since the middle of the last century, seismic ambient noise has been considered a valuable source of information for the investigation of the shallow subsurface structure. Among other methods, the horizontal to vertical spectral ratio (HVSR or H/V) method (Nakamura, 1989), gained extreme popularity, especially in the last decades in fields such as geology, geotechnics, seismology and recently even in archaeology (Wilken et al., 2015; Abu Zeid et al., 2016, 2017), both because of its simple approach and because it only requires low cost equipment.

The HVSR method is based on recording the three components of the seismic noise which are then Fourier transformed and smoothed. The spectral ratio of the horizontal to vertical component then, constitutes the so called HVSR curve. The main assumption for the interpretation of such curves is that the subsurface can be well described as a soft sedimentary layer (with low shear wave velocity, or V_s) lying over a fast bedrock. In general, both the layer and bedrock are considered homogeneous and viscoelastic, while the seismic noise is assumed to be isotropic. In such a simplified (1-D) model, the correlation between elastic properties, thickness of the sedimentary layer and frequency position of the curve's peaks, has been demonstrated. For example, Lachet and Bard (1994) used a uniform distribution of point-wise sources to numerically simulate the seismic noise in an urban context while Bonnefoy-Claudet et al. (2006) estimated the effect of different sources on the resulting wavefield. Being an extremely popular topic, the related literature is quite abundant and the interested reader could refer to the study by Bard (1998) who presents an overview of the HVSR method, Mucciarelli and Gallipoli (2001), and Deliverables D13.08 (2004), D23.12 (2005) of the European project SESAME.

As recalled by Guéguen et al. (2007), the method is used mainly for three different scientific purposes, namely the evaluation of the resonance frequency as correlated to earthquake damage, the investigation of the resonance variation over large areas for microzonation and seismic-risk mitigation purposes and finally, for evaluating the thickness of the sedimentary cover or equivalently, the depth of bedrock.

Among the three, the evaluation of the sedimentary thickness surely represents the most recent application, so that only a few papers have been published in this area (Ibs-von Seht and Wohlenberg, 1999; Delgado et al., 2000; Parolai et al., 2002; Hinzen et al., 2004; Garcia-Jerez et al., 2006; Motamed et al., 2007; D'Amico et al., 2004;

* Technology Square Research Building, Office 403, 85 5th St NW, Atlanta, GA 30308, USA.
E-mail address: bgnsml@unife.it.

http://dx.doi.org/10.1016/j.jappgeo.2017.07.017
0926-9851/© 2017 Published by Elsevier B.V.

Abu Zeid et al., 2014). The bedrock depth (H) could in principle be evaluated using a very simple approach based on the ratio $H = f_0/\overline{V_s}$ between the main resonance frequency f_0 and the average shear wave velocity $\overline{V_s}$ of the sedimentary cover. However, since the problem is posed as an equation with two unknowns, an estimate of the average $\overline{V_s}$ is required. As I will discuss later, this strategy is oversimplified and may lead to severe errors. A preferable approach was described by Ibs-von Seht and Wohlenberg (1999). In their pioneering work, they showed that it is possible to map the thickness of the sedimentary cover by either using an approximate local estimate of the subsurface velocity profile or alternatively, by simply establishing a two-parameters (a,b) regression (sometimes referred to as a calibration function or correlation equation), of the form $H = af_0{}^b$ which is built using the bedrock depth measured at some existing wells and the resonance frequency f_0 at the well's top, which is obtained by the HVSR method. In their experiment, Ibs-von Seht and Wohlenberg had wells available for roughly 34% of the HVSR measurements. Of course, the regression is valid only at the investigated site; but once established it is possible to infer the sediment thickness within the entire survey area, provided that the V_s profile presents negligible lateral variation across the surveyed area. It is noteworthy that the calibration function is experimentally determined and does not require an explicit knowledge of the V_s profile. According to experimental evidence, the method proved to be capable of estimating the bedrock depth from shallow targets (<50 m) up to hundreds of meters deep (deep bedrock case).

Delgado et al. (2000) examined in depth the theoretical basis of Ibs-von Seht and Wohlenberg's approach in order to better establish the limitations of the method. They concluded that this tool can efficiently be used to retrieve the bedrock depth at locations where this information is missing. Further, as their work was entirely based on field data, they defined the constants of the calibration function for the Bajo Segura Basin (Spain). The bedrock ranged between 15 and 60 m in depth, so their work represents an example of a shallow bedrock situation. Despite the fact that the true sedimentary cover was actually a multi-layered system, which they approximated with just two layers, and despite the topmost sediments were not accounted for, they found that the error in evaluating the bedrock depth was only of on the order of 15% once compared with the available detailed geotechnical information. In this way, they experimentally demonstrated that the general approach is very robust. Further, they discussed different sources of uncertainty that may affect the depth estimates and addressed local lateral subsurface deviations from the assumed velocity profile as the main source of error.

Using Ibs-von Seht and Wohlenberg's regression, Parolai et al. (2002), found a systematic underestimation (up to 30%) in the thickness estimates performed in the Cologne area (Germany), with the largest error corresponding to those areas of deepest bedrock. They concluded that the Ibs-von Seht calibration curve was not suitable for the study area and derived a new set of parameters capable of reducing such error.

Gosar and Lenart (2010) gave a comprehensive overview of the regression parameters values encountered in literature. Further, they applied the method for the Ljubljana Moor Basin (Slovenia). They had a good availability of wells and their $f_0 - H$ regression was based on 53 unevenly distributed wells. Such regression was then used to retrieve the bedrock depth along an independent profile. They gave a detailed discussion about experimental uncertainties mainly addressing 2D and 3D effects due to the basin geometry and local lateral variations. Further, they pointed out the presence of side peaks as an indication of the presence of a complex subsurface structure.

Finally, Johnson and Lane (2016) compared different methods of evaluating the thickness of sediments using field data and a statistical approach. They investigated a shallow bedrock case (depth ranged between 1 and 60 m), and in that context, they compared the bedrock depth obtained by a purposely derived calibration function, two published calibration functions and the one obtained using the simplified constant V_s approach (Eq. (2)). Noteworthy, from their work it can be observed that the bedrock depth obtained using the constant average V_s approach, when compared to that obtained by the ad-hoc produced calibration function, is systematically underestimated. The underestimation increased with depth reaching roughly 15% in the worst case scenario.

Judging from published experimental evidence, therefore, it is quite established that this application of HVSR is very robust, provided that a purposely built calibration function is available for the site at hand (see for example Table 2 in Appendix B). Evaluation of experimental uncertainties shows that in general, when compared with wells data, the error in bedrock depth estimates is lower than or at least comparable to 15%. Authors have justified this discrepancy invoking different sources of uncertainty with local lateral variation of elastic properties as the most popular one, despite the lack of formal proof. Since experimental evidence about the success of the method and its degree of uncertainty are already very convincing, the purpose of this paper is not the evaluation of uncertainties through the study of further experimental datasets. I will rather investigate the lateral variation exclusively from a modeling point of view.

The way a lateral variation changes the outcome of the bedrock depth estimation is that a slight local change in subsurface elastic properties results in a small shift of the resonance frequency. We can then imagine the lateral variation as a small perturbation of our reference model, compute the resonance frequency of the perturbed model and evaluate how the frequency shift affects the estimated depth. Since for a given reference model there are an infinite number of possible perturbations, a statistical approach must be used.

To accomplish this I used a modified version of the code OpenHVSR v2.0 (Bignardi et al., 2016; Herak, 2008), which allows the simulation of HVSR curves either considering the contribution of body waves, implemented using Tsai and Housner's approach (Tsai, 1970; Tsai and Housner, 1970) and surface waves, through the approach implemented by Lunedei and Albarello (2010) as the formation mechanism. Indeed, it was demonstrated (Nakamura, 2000; Bonnefoy-Claudet et al., 2006) that the seismic noise may contain contributions from both multiple refracted body waves and surface waves; so that, for consistency, both formation mechanisms must be investigated. Two different multi-layered subsurface scenarios are used as reference. The first is a multi-layered system with a constant V_s profile, while the second implements the same velocity-depth distribution discussed in the paper by Ibs-von Seht and Wohlenberg (1999), which is a normally dispersive model (i.e. velocity increases with depth) accounting for the confinement pressure increasing with depth. The investigation is performed by using the Monte Carlo method (MC) to produce a statistically meaningful number of perturbations of the reference models. I randomly perturbed both the V_s and V_p profiles evaluating the impact of the introduced perturbation on the resonance frequency and the consequent impact on the estimated thickness of sediments. In the following the strategy to conduct this study will be introduced and the results carefully commented. For sake of clarity, however, results are also summarized Appendix B (Table 1), and compared with published experimental uncertainties (Table B.2). Conclusions will follow.

2. Material and methods

All tests performed here were realized using an ad-hoc modified version of the program OpenHVSR (Bignardi et al., 2016) specifically designed for bedrock depth evaluation purposes. Each test investigated a different reference subsurface configuration. The first one (Table A.1) built using a constant V_s profile subdivided in 5 layers, each one 8 m thick, simulates a soft sedimentary cover lying over a hard half space. Two different sets of models were produced by perturbing this reference subsurface in order to obtain a set of normally dispersive and a set of inversely dispersive models (i.e. velocity decreasing with depth), all produced by keeping the thickness of layers constant.

Table 1
Regression parameters *a* and *b* published in different case studies as compared with those numerically computed in this investigation.

Site	Regression	*a*	*b*
Cologne (Germany)	Parolai et al. (2002)	108.0	−1.551
Lower Rhine-east (Germany)	Hinzen et al. (2004)	137.0	−1.190
Lower Rhine-west (Germany)	Ibs-von Seht and Wohlenberg (1999) field data	96.0	−1.388
	Ibs-von Seht and Wohlenberg (1999) theoretical	111.52	−1.3677
This study	Body waves (Tsai…)	133.41	−1.2615
	Surface waves (Picozzi…)	140.40	−1.4077

Consequently, the depth of bedrock was fixed at 40 meters depth. As such, this represents a shallow bedrock scenario. Perturbations consisted of changing the V_s velocity of each layer by a random amount, up to 50% variation with respect to the original value under the requirement that the whole perturbed profile must present the same average V_s as the reference model, when calculated according to

$$V_{ave} = \frac{\sum_i H_i}{\sum_i \frac{H_i}{V_i}}, \tag{1}$$

where H_i and V_i are the thickness and velocity of the ith layer respectively. Prior to being applied, perturbations were ordered in ascending or descending order to generate the normally or inversely dispersive behavior.

When the subsurface can be described with one whole slow layer over a fast half space, the elastic wave equation can be analytically solved in term of resonance frequencies. The quite popular solution states that the HVSR curve shows many peaks occurring at the resonance frequencies of the system (Lanzo and Silvestri, 1999). Further, these frequencies only depend on the shear velocity V_s and thickness H of this single layer (Eq. (2))

$$f_{(n)} = \frac{V_s}{4H}(2n-1), \tag{2}$$

where n indicates a specific peak of the HVSR curve. If the half space is partially adsorbing, the amplitude of the peaks is decreasing when n increases, so that usually, only the main peak ($n=1$) is considered. This disarmingly simple result is easily proven by assuming the multiple reflection and refraction of shear waves (Lanzo and Silvestri, 1999). Of course, if the V_s profile can be determined, Eq. (2) could, in principle, be used to infer the depth of bedrock, and if multiple measurements are available over the same area, the bedrock may even be mapped.

However, from a modeling point of view, the subsurface is better described as a stack of layers with properties changing with depth which in turn requires enforcing stress and displacement continuity conditions at the interfaces between layers. For this reason, the solution of a multilayered system is inherently different when compared to the solution of the unique-layer over half space model and HVSR curves must be computed numerically. It could be argued that the effect of such interface conditions is negligible when the change in elastic properties is small, and especially, when such changes are small compared with the abrupt elastic impedance contrast at the sediments-bedrock interface. This is a reasonable observation, and as a matter of fact, many authors use Eq. (2) to obtain a rough evaluation of the bedrock depth. Yet, to my knowledge, no theoretical investigation has been carried out in this direction. Therefore, the purpose of my first test is to numerically quantify the expected deviations which may affect the bedrock depth estimate when the latter are performed by the simple but arguable application of Eq. (2).

My second test concerns the evaluation of the impact of subsurface deviations from a defined reference model, which is represented by a more sophisticated subsurface built using a V_s profile defined through Eq. (3)

$$H = \left[\frac{V_0(1-x)}{4f_r} + 1\right]^{1/(1-x)} - 1, \tag{3}$$

which relates the thickness of sediments H to the resonance frequency f_r and accounts for the increase of V_s with depth due to the increasing confining pressure. I set $V_0 = 162$ m/s as the shear wave velocity at the surface and $x = 0.278$ as depth-weighting constant so obtaining the same model investigated by Ibs-von Seht and Wohlenberg (1999). Further, the V_p profile is built to account for both the augmented velocity with depth and to accommodate the water table (WT). See Tables A.2 and A.3 for details. Ibs-von Seht and Wohlenberg demonstrated that by knowing the bedrock depth at a sufficient number of locations (through wells or other geophysical methods) and computing the main resonance frequency by the HVSR method at the same locations, a regression of the form $H = af^b$ can be built. Such regression can then be used to map the sediment thickness over the entire areas under investigation, without the need of determine the V_s profile, provided that the shear velocity profile obeys a relation similar to Eq. (3) and without lateral variations.

Therefore, as a first step, I evaluated the parameters a and b for the reference model described by Eq. (3) simulating the HVSR curves for different bedrock depths, under both the assumption of the body and surface waves formation mechanism. The result is compared with Ibs-von Seht and Wohlenberg's original work and other published analogous work in Table 1.

I recall that the purpose of this second investigation was to evaluate the amount of uncertainty, due to a lateral variation, which could affect the sediments thickness evaluation. According to published work, such uncertainty depends both on the depth at which the real subsurface deviates from the assumed model and on the depth of bedrock. Since in the majority of publications regarding this topic the assumption of no lateral variation is a good approximation for the most part of the measurement locations, it seems reasonable that such variations take the form of a local lens having changed elastic properties. Following these considerations I investigated two cases in which the bedrock lies 750 and 50 m deep, which represent deep and shallow bedrock scenarios respectively. The subsurface for the two scenarios was subdivided respectively into 32 and 18 layers and successively used to generate six different sets of perturbed models each. The effect of shallow, middle-depth and deep perturbations was investigated by changing the velocity values in the topmost, central and deep portion of layers respectively.

Further, to simulate the effect of a lenticular body crossing the model under the measurement point, each velocity perturbation was built by generating random values with normal distribution and ordered so as to obtain a vector of values with the maximum in the middle position and symmetrically fading. Such perturbation was then added to or subtracted from the velocity values of the portion of layers at hand to investigate both the velocity underestimation and overestimation. For clarity sake, a few selected perturbed models are shown later in Fig. 4. The same strategy was used both to modify V_s and V_p.

However, two independent perturbation vectors were generated each time as I wanted to keep V_p and V_s uncoupled. Indeed, despite the fact that the V_p parameter has a weak effect on the HVSR curve when compared to V_s (Bignardi et al., 2016), its importance should not be overlooked. In particular, I introduced the water table effect as a constant $V_p = 1500$ m/s extending from the shallow layers to a depth where this value was reasonably exceeded.

Finally I allowed a maximum layer-wise variation of 50% for velocities, while density and quality factors were kept constant. All parameters of the bedrock were kept fixed as well.

Of course, every perturbed subsurface presented slightly changed average values of both V_s and V_p with respect to the reference model, and consequently, slightly different resonance frequency. Therefore, the percent change in average V_s was correlated to the percent change in the resonance frequency. Further, the error in evaluating the bedrock depth was estimated and correlated to the average V_s as well.

The chosen amount of perturbations could not entirely change the nature of the model defined by Eq. (3), so that the perturbed models retained an almost normally dispersive trend in nature. Consequently, I classified different sets of simulations based on the characteristics of the perturbation used: "shallow", "middle-depth" and "deep", depending on the position of the affected layers, and "+", or "−" when velocities were increased or decreased.

Concerning the modeling routines I used, since the computational time required to run the surface waves-based one is consistently slower than the body waves-based one, the number of perturbed models I produced using the first is smaller with respect those produced using the second one. Therefore, in both the first and second test, the datasets related to body waves comprised 50,000 subsurface perturbations while the simulation of surface waves comprised 5000. As a final consideration regarding test 2; it could be argued that, the use of modeling routines based on a subsurface described by a stack of flat layers to investigate lateral variations seems like a contradiction. Indeed, such approach is only valid under the assumption that the local lateral variation is small compared to the wavelength associated to the main peak, which is indeed the case of the present simulation, as the perturbed portion of the subsurface spanned over few layers.

3. Results

3.1. Test one

In my first test, the subsurface model of Table A.1 was perturbed using the MC approach in order to produce two different sets of models. I investigated a set of perturbations where the resulting subsurface is strictly normally dispersive and a second set which is strictly inversely dispersive (Fig. 1c). Since the V_p profile has a weak, but not negligible impact on the main peak position, each time a V_s subsurface is created, a corresponding V_p profile is created using an extra MC run. This allowed an investigation of the perturbed models with variable V_p/V_s ratios so that the final result of the investigation is free from effects that may be addressed to a systematic use of a linear dependence between the two elastic parameters. As a perturbed subsurface generates an HVSR curve with a main peak slightly changed in position, only a limited range of frequencies need to be investigated. Fig. 1a and b show the HVSR curve obtained considering body and surface waves respectively. The response of the reference model for body waves with or without the presence of the water table is represented by the thick solid and the narrowly dashed lines respectively, while the loosely dashed line corresponds to the response of surface waves.

The curves obtained for the normally and inversely dispersive perturbed models are shown in black and gray respectively. Since the modeling was performed enforcing the same average V_s (according to Eq. (1)), the effects shown in Fig. 1 only depend on the velocity gradient. In particular, the frequency of the main peak is systematically overestimated when the subsurface becomes a multilayered normally dispersive system and systematically underestimated in the inversely dispersive case. Notably, the behavior seems to be accentuated for the surface waves which in this particular subsurface configuration may undergo a jump of peak, i.e. a peak that is secondary for the reference model becomes dominant for the perturbed subsurface. Despite the fact that microtremor may be well described by a diffuse field (stochastic in nature) the effect may be thought as related to a change of the dominant propagation mode or to a change in waves ellipticity, effects which are known to be likely when lateral variations come into play (Bignardi et al., 2014; Cercato, 2015) Fig. 2a shows the percent difference between the frequency peak positions of the perturbed models with respect to the expected value, as a function of the average velocity gradient of the corresponding subsurface.

When the subsurface is normally dispersive, the deviation is almost always bounded under 30%. For the inversely dispersive case, body waves mostly lead to a deviation under 35%, but in some cases it is

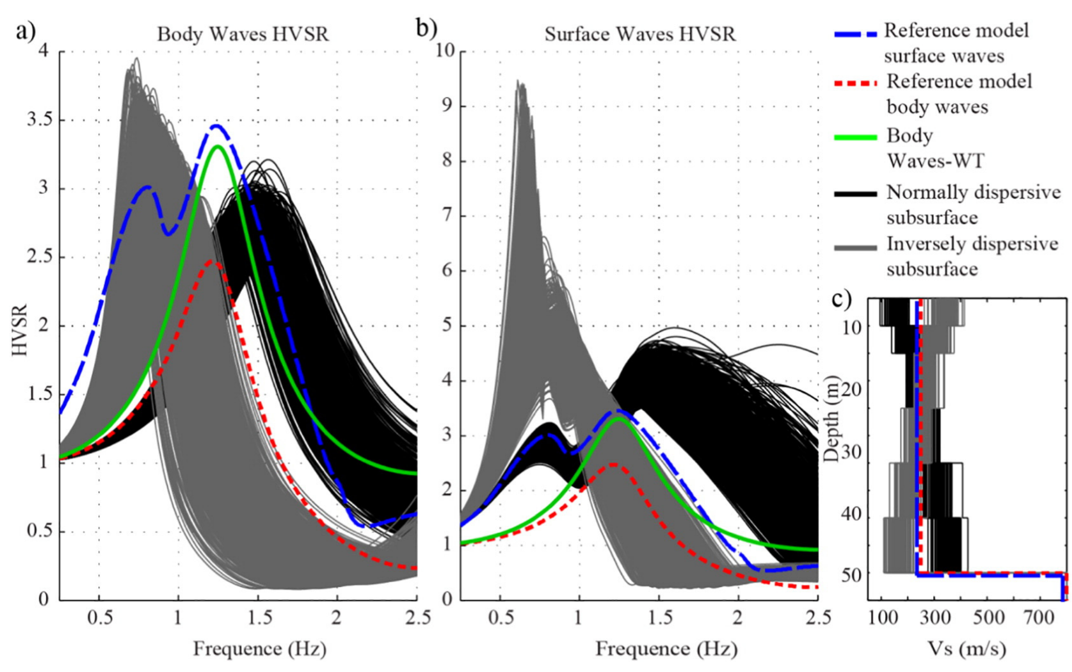

Fig. 1. HVSR curves simulated using the propagation of body and surface waves are shown in figures a) and b) respectively. The reference model response when the body-waves formation mechanism is considered is shown with a solid and a narrowly dashed line, depending if the water table effect is included or not, while the response of surface waves (water table included) is shown with the loosely dashed line. The sets of black and gray lines represent the responses of normally and inversely dispersive subsurface models respectively. All the investigated models share the same depth to bedrock (H) and the same average V_s. Finally, figure c) shows an example of the V_s values spanned by both the normally and inversely dispersive subsurface.

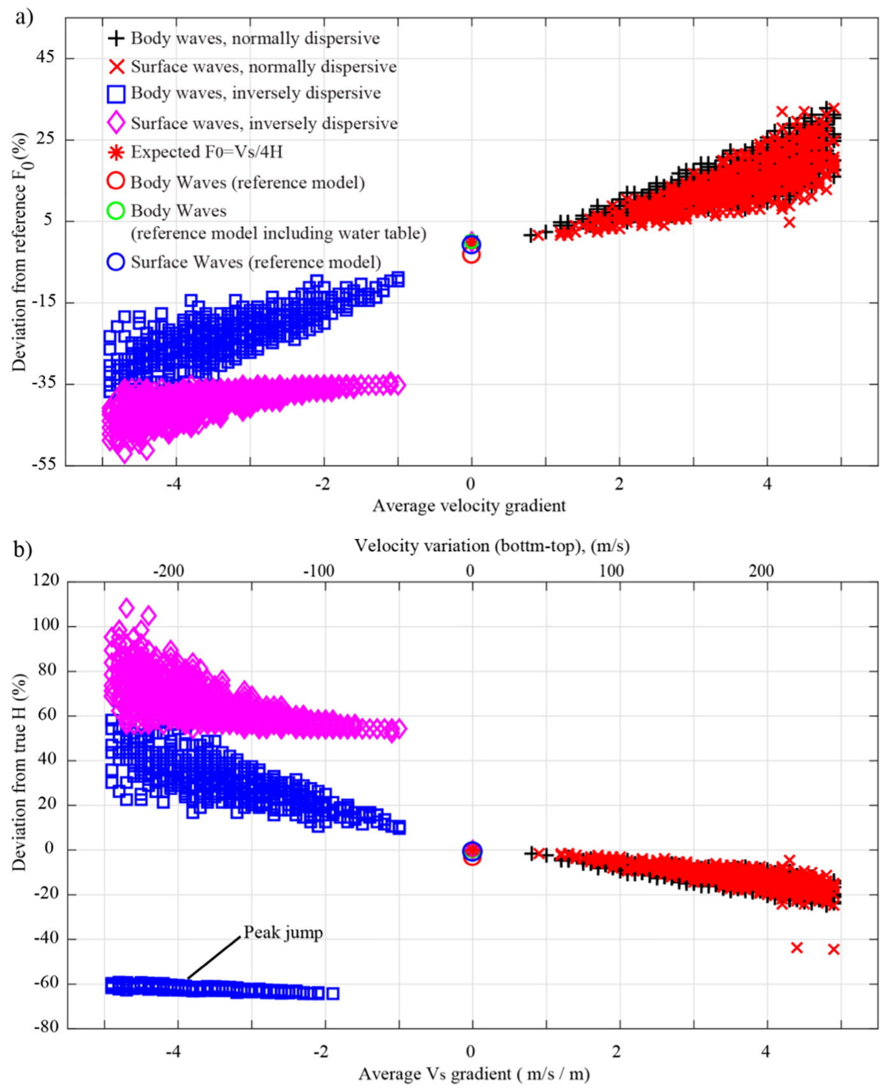

Fig. 2. a) Percent deviation of the fundamental resonance frequency with respect to the expected value (i.e. the reference model response) produced as effect of the velocity perturbation. Such deviation is shown as function of the average V_s gradient. Positive and negative velocity gradients correspond to normally and inversely dispersive subsurface respectively. b) Percent deviation in estimated sediment thickness with respect to the known value is shown as a function of both the average V_s gradient (scale at bottom) and as a function of the net V_s difference between the bottom and the top sediments (scale on top).

possible for the main peak position to change abruptly. The effect on thickness error is shown in Fig. 2b. Surface waves, as it can be noted, are greatly affected by the inversely dispersive subsurface.

Fig. 2b shows the percent difference in estimated sediment thickness (using Eq. (2)) with respect to the known value as a function of both the average V_s gradient (scale at bottom) and as a function of the velocity difference between the bottom and the top of sediments (scale on top).

For the normally dispersive subsurface case, the error in subsurface sediments thickness evaluation is mostly under 30%, even in the most extreme case.

For inversely dispersive models, body waves lead to an error under 20% only when the inversion is weak while in cases of strong inversion may lead to an error up to 40–60% or to abrupt changes of main peak position and consequently the sediment thickness may be severely mistaken. It is worth mentioning that the latter conclusion only apply when the whole profile is inversely dispersive which seldom happens in real soils, while the case of inversion limited to few layers, as it will be show in the following, behaves much more regularly. It is worth noting that when the constant V_s subsurface is used as reference and we change toward a normally dispersive one, the consequence is depth underestimation. Conversely, if the normally dispersive subsurface is taken as the true model, switching toward a constant V_s one results in depth overestimation. This is exactly what was experimentally obtained by Johnson and Lane (2016) who found that the constant V_s approach lead to a shallower bedrock depth when compared to that obtained by the Ibs-von Seht and Wohlenberg-like regression.

3.2. Test two

As first part of my second test, the V_s profile of Eq. (3) was used to computationally obtain the parameters *a* and *b* of the Ibs-von Seht and Wohlenberg fashioned regressions shown in Fig. 3.

In the second part of the present investigation, a Monte Carlo algorithm was used to obtain, from the two models of Tables A.2 and A.3, three different sets of perturbed models by perturbing a portion (one third) of the layers at time. The first, second and third set were obtained by perturbing the shallow, middle and deep portion respectively. The perturbation strategy consisted in slightly changing both V_s and V_p to obtain a perturbation symmetric with respect to the perturbed section with its maximum change in the middle and fading toward the edges (few selected examples are shown later on, in Fig. 4). Such perturbations were either added or subtracted in order to investigate

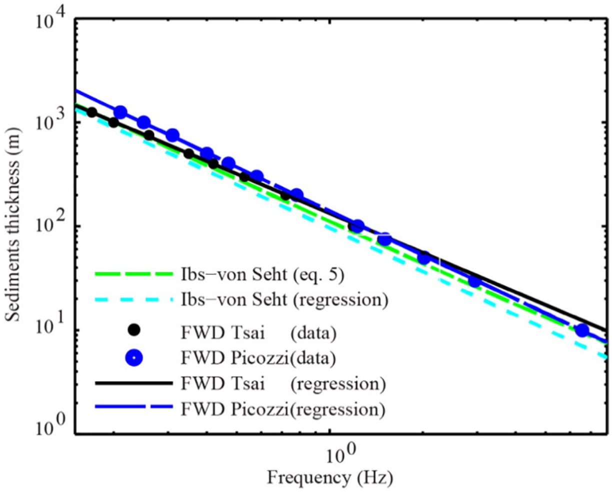

Fig. 3. Comparison between regressions. Ibs-von Seht and Wohlenberg's analytical calibration curve (Ibs-von Seht and Wohlenberg, 1999, Eq. (5)) and empirical regression are compared with the regressions obtained in this study and simulated (f_r,H) points, as obtained for Ibs-von Seht and Wohlenberg's (1999) subsurface model (Eq. (3)) and computed assuming both the body and surface waves propagations as formation mechanisms. The regressions based on body and surface waves propagation are drawn in solid black and loosely dashed blue respectively. Such regression lines are based on specific simulations highlighted with circles in the figure and performed using Tsai and Housner's approach (for body waves) and Picozzi and Alarello's approach (for surface waves). Ibs-von Seht and Wohlenberg's regressions are shown alongside for comparison. Finally, values for a and b constants for different regressions commonly encountered in literature are listed in Table 1. (For interpretation of the references to color in this figure legend, the reader is referred to the web version of this article.)

both the cases of velocity overestimation and underestimation. Fig. 5a and b, related to the case of shallow bedrock (50 m deep), show the percent error in evaluating the sediment thickness as compared to the average V_s velocity of the entire stack of layers and to the maximum layer-wise variation.

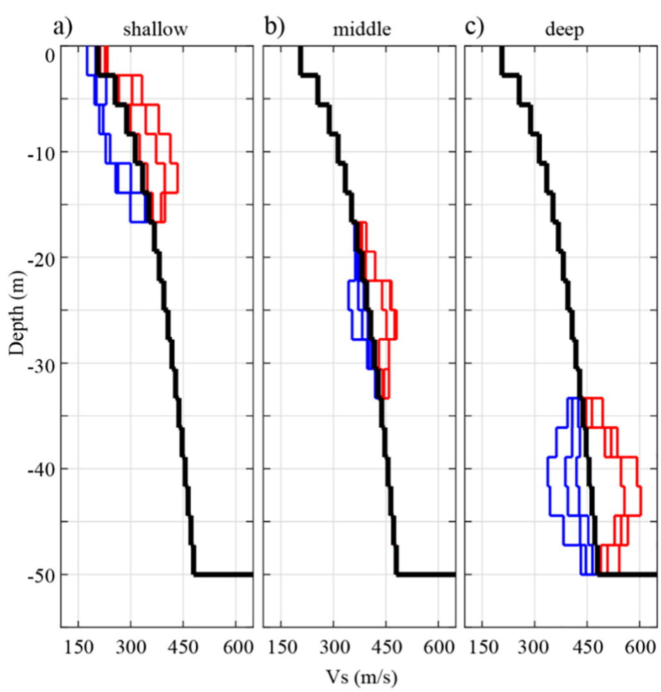

Fig. 4. Range of subsurface velocity perturbations (shallow bedrock case), designed to study the dependence of the error in bedrock depth evaluation. Selected examples of shallow, middle-depth or deep velocity perturbations are shown in figures a, b, c respectively.

Note that, in this example the sediment thickness was evaluated, congruently with Ibs-von Seth and Wohlenberg's approach, using the regression previously obtained (Fig. 3).

The result for all of the three subsurface sections and for both the velocity underestimation and overestimation scenarios is plotted. It can be noted that, in general, the average V_s variation is under 20% and in this range when the average velocity is increased, the percent error is under 15%. On the other hand, in case of velocity underestimation, the error is still limited but can be higher. The cases of shallow, middle-depth and deep perturbation show a similar behavior, except that the effect is stronger when the varied layers are deeper. This is because even if a generic change of V_s affects the whole profile, when such change is deeper it has a greater effect on low frequencies where the resonant peak usually lies. Shallow perturbations, on the other hand, affect mostly (but not only) the high frequency part of the curve. Surface waves and body waves formation mechanisms behave coherently. Fig. 5b shows the estimated percent error in sediment thickness as a function of the maximum percent layer-wise change. It seems that to obtain an error of about 15%, a subsurface V_s variation higher than 25% is required. Bearing in mind how the lens was simulated in this study, such variation can be considered rather strong, and this explains why the errors addressed to lateral changes in the literature are usually of the order of 15% or less.

Finally, for sake of completeness, Fig. 6 relates the percent change in average V_s velocity with the percent maximum layer-wise variation. It can be noted that the impact on the average V_s of changing the V_s of few layers is modest even when such change is consistent.

As a result Ibs-von Seht and Wohlenberg's approach results particularly stable against local lateral variations. Figs. 7 and 8 show the analogs of Figs. 5 and 6 in the case of deep bedrock (750 m).

The same considerations made for the shallow bedrock case hold except the effect of perturbing the shallow portion of the velocity profile is rather limited, as could be expected. Such low impact of the shallow part of the velocity profile explains why Delgado et al. (2000) were able to overlook the topmost soil without affecting their final result.

For the deep bedrock case, the error related to surface waves seems to be slightly higher than the one obtained for body waves. However, such a difference could be simply due to the different computational approach implemented in the forward modeling routines and it seemed not sufficiently pronounced to suggest any special physical interpretation. As was pointed out in test 1, the use of the simplified approach of Eq. (2) for the determination of H, even calculating the average V_s from the true profile (Eq. (1)), always led to underestimation. The error, both considering body or surface waves, was about 9% for the shallow bedrock case, while was of 3% (body waves) and 22% (surface waves) for the deep bedrock scenario.

4. Conclusion

It is known from experimental evidence that the HVSR method has proved to be successful for mapping the thickness of sedimentary covers laying over consolidated bedrock.

The simplest approach based on constant V_s (Eq. (2)) reveals to be an oversimplified strategy which on the most common realistic case, i.e. a normally dispersive subsurface with V_s increasing with depth, may lead to systematic underestimation of the bedrock depth on the order of 15–25%. This conclusion was shown by experimental evidence in the work by Johnson and Lane (2016). Conversely, when the subsurface is entirely inversely dispersive, the error may easily exceed 20%. Further error may arise when a secondary peak exists because such a peak may become dominant as a result of the lateral variation. Despite the fact that only a “shallow bedrock” scenario was investigated, my results point out that the use of the simplified approach of Eq. (2) should be used with care and only to gain a rough understanding of the subsurface.

A far more elegant and reliable approach was described by Ibs-von Seht and Wohlenberg (1999), in which a site dependent calibration

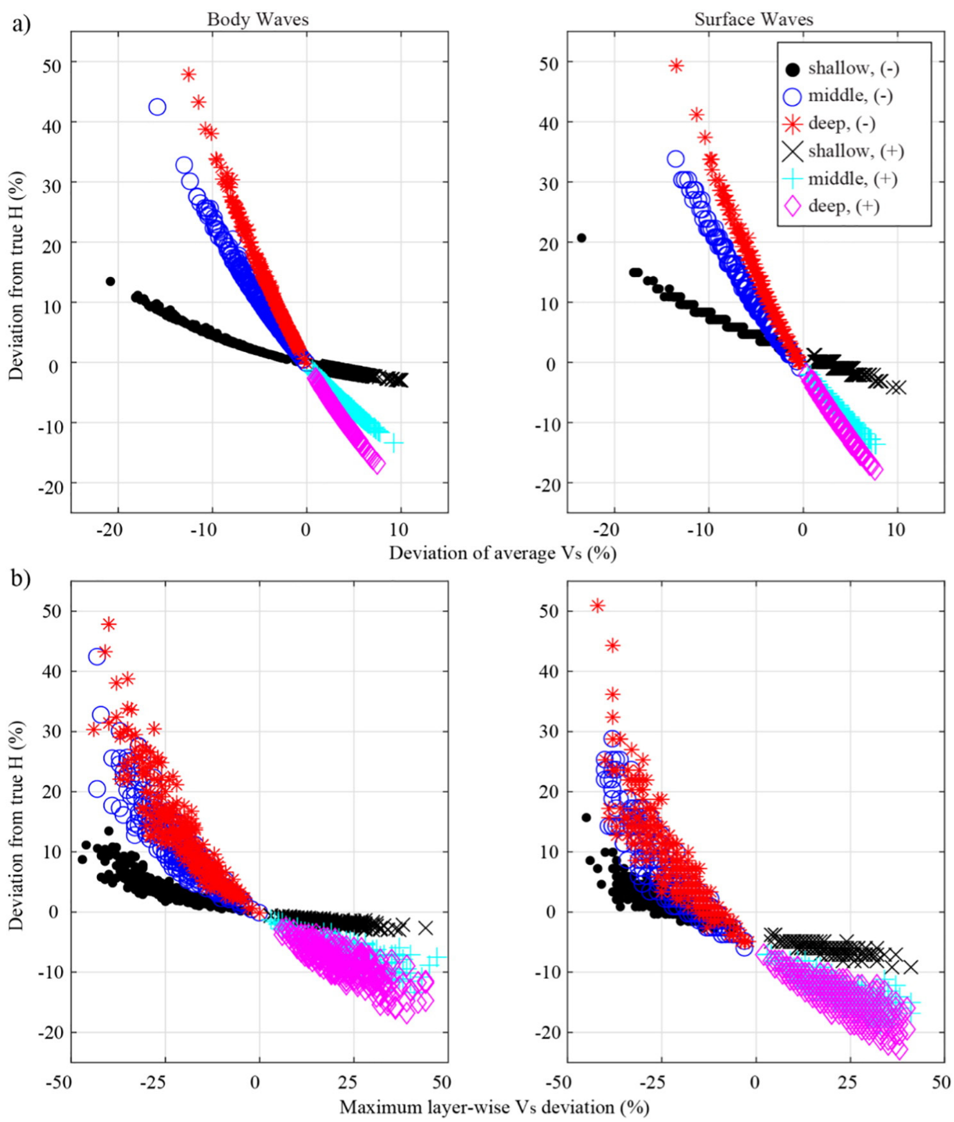

Fig. 5. The percent difference between the bedrock depth evaluated using the HVSR main peak and the computed regressions (Fig. 3), and the true value (50 m), is shown as a function of the average V_s of the subsurface (a) and as a function of the maximum layer-wise V_s perturbation (b). Effects of both body and surface waves formation mechanisms were investigated.

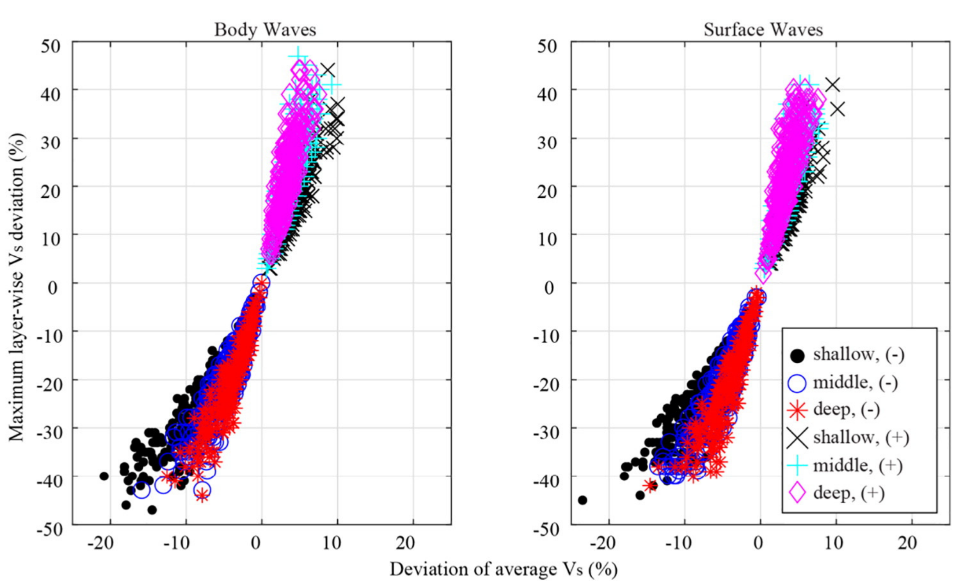

Fig. 6. Average V_s of the subsurface as a function of the maximum layer-wise V_s perturbation for a bedrock 50 m deep.

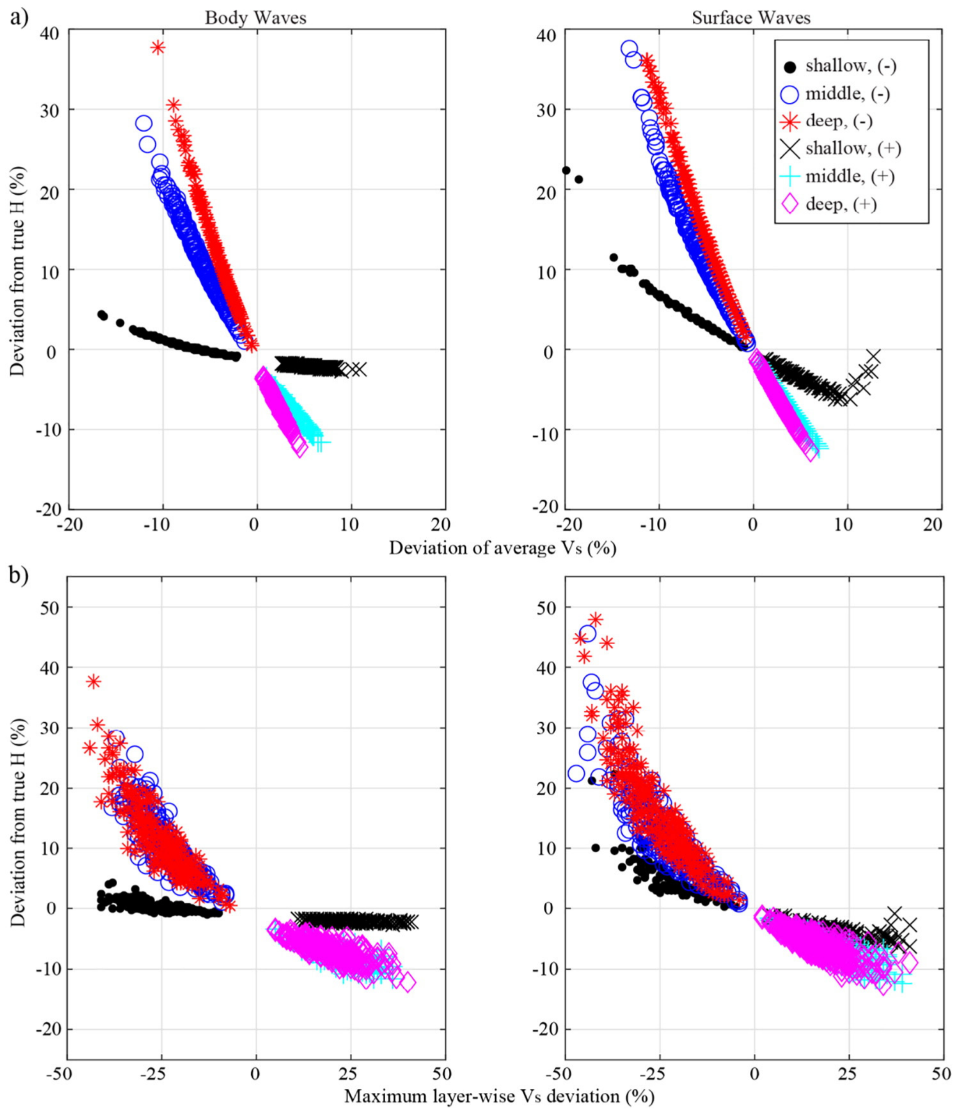

Fig. 7. The percent difference between the bedrock depth evaluated using the HVSR main peak and the computed regressions (Fig. 3), and the true value (750 m), is shown as a function of the average V_s of the subsurface (a) and as a function of the maximum layer-wise V_s perturbation (b). Effects of both body and surface waves formation mechanisms were investigated.

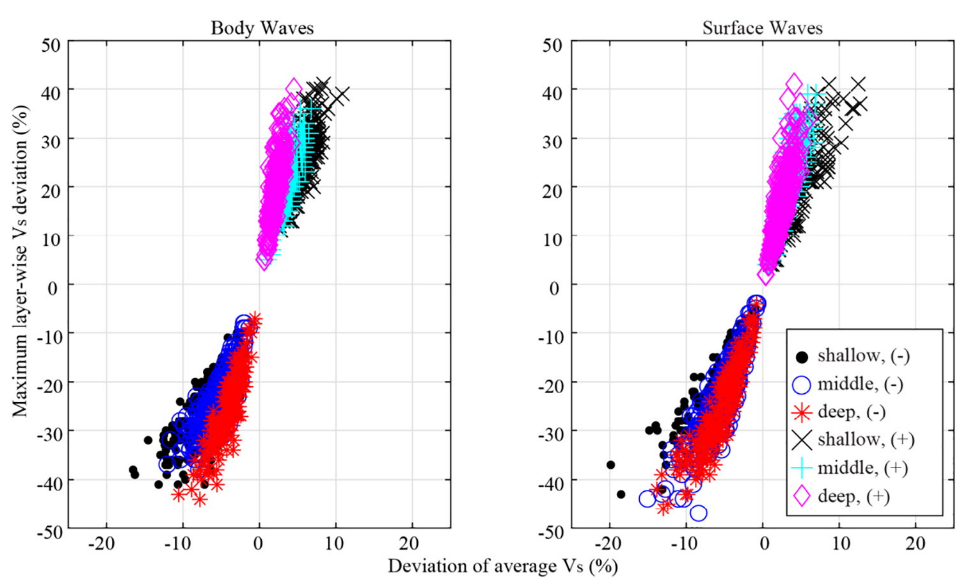

Fig. 8. Average V_s of the subsurface as a function of the maximum layer-wise V_s perturbation for a bedrock 750 m deep.

function is built and used for the bedrock depth estimation. I numerically computed the theoretical calibration functions for both the cases in which the HVSR curve is to be considered as the outcome of multiple reflected and refracted body waves or as the result of surface waves propagation. Despite the fact that two independent modeling routines and two independent formation mechanisms were considered, the result, computed for the same subsurface model revealed to be very similar to that proposed by Ibs-von Seht and Wohlenberg. Since in this contest, among the various sources of uncertainty that can affect the sedimentary thickness estimation, the local deviations from the assumed model have been suggested by many authors as the most contributing factor, I numerically investigated this aspect for the Ibs-von Seht and Wohlenberg's subsurface model taking into account shallow (50 m) and deep (750 m) bedrock scenarios. In both cases the introduction of localized perturbations in soil velocities produced results in line with the experimental observations. In particular, the deeper the perturbation, the stronger was the resulting error on thickness. Further, an increase (decrease) of V_s systematically led to depth underestimation (overestimation).

I verified that, in both cases, subsurface variations capable of changing the average V_s up to 10% may at most introduce errors of 20% or less in the bedrock depth. Such a modest change in average V_s, however, may be accompanied to strong layer-wise variations. The latter consideration, points in the direction that Ibs-von Seht and Wohlenberg's approach is very robust when the subsurface abides by the basic assumptions of the method.

It is noteworthy that for a normally dispersive subsurface, an increased V_s at depth leads to an underestimation of sediments thickness while when the V_s at depth is decreased, the sediment thickness is overestimated. However, in all the cases I investigated (i.e. layer-wise perturbation up to 50%, resulting in an average V_s change under 20%), when the deviation of average V_s is reasonable, the error is always below 20%. No simple relation between the deviation of the average V_s and the error in estimation of the bedrock depth could be found, however, the simulation approach herein proposed represents a useful tool to evaluate the reliability of a bedrock depth estimated from real data. Such a tool accompanied by the HVSR inversion enables one to assess the reliability of the estimated depth through the stochastic investigation of the parameters space around the reference model and may reveal a very convenient tool when lateral variations are suspected or the number of available wells is not sufficient to obtain a good regression. The opportunity of using the modeling/inversion tool for such purposes will be discussed in a forth coming paper.

Acknowledgements

The author would like to thank Prof. Giovanni Santarato, Prof. Riccardo Caputo, and Prof. Nasser Abu Zeid, at the University of Ferrara (Italy) for their useful suggestions and for the stimulating discussions on the topic, and Ph. D. Robin Yezzi for the preliminary revising. The author would also like to thank the anonymous reviewers for their valuable suggestions on how to improve the final manuscript.

Appendix A. Subsurface models

Table A.1
Properties of the sediments and rocky half space used in test 1 are listed. During modeling, the 40 m thick sedimentary cover was subdivided into 5 layers each one 8 m thick. For sake of comparison with analytical solution (Eq. (2)), the model was considered purely elastic so that quality factors Q_p and Q_s were set up accordingly.

Layer	*H* (m)	V_p (m/s)	V_s (m/s)	Rho (?)	Q_p	Q_s
Sedimentary	40	600	250	1.8	n.a.	n.a.
h.s.	n.a.	2000	800	1.8	n.a.	n.a.

Table A.2
Visco-elastic subsurface properties used in test 2 to simulate a deep bedrock scenario.

Layer	*H* (m)	V_p (m/s)	V_s (m/s)	Rho (g/cm^3)	Q_p	Q_s
1	10	426	267	1.8	30	15
2	20	1500	377.7	1.8	30	15
3	20	1500	454.9	1.8	30	15
4	25	1500	513.7	1.8	30	15
5	25	1500	563.3	1.8	30	15
6	25	1500	603.7	2	30	15
7	25	1500	638.0	2	30	15
8	25	1500	668.1	2	30	15
9	25	1500	695.1	2	30	15
10	25	1500	719.6	2	30	15
11	25	1500	742.1	2	30	15
12	25	1500	762.9	2	30	15
13	25	1500	782.4	2	30	15
14	25	1500	800.7	2	30	15
15	25	1500	818.0	2	30	15
16	25	1500	834.3	2	30	15
17	25	1500	849.9	2	30	15
18	25	1500	864.8	2	30	15
19	25	1500	879.0	2	30	15
20	25	1500	892.6	2	30	15
21	25	1500	905.8	2	30	15
22	25	1500	918.4	2.2	30	15
23	25	1500	930.7	2.2	30	15
24	25	1508	942.5	2.2	30	15
25	25	1526	953.9	2.2	30	15
26	25	1544	965.0	2.2	30	15
27	25	1561	975.8	2.2	30	15
28	25	1578	986.2	2.2	30	15
29	25	1594	996.4	2.2	30	15
30	25	1610	1006.4	2.2	30	15

Table A.2 (*continued*)

Layer	*H* (m)	V_p (m/s)	V_s (m/s)	Rho (g/cm^3)	Q_p	Q_s
31	25	1626	1016.0	2.2	30	15
h.s.	n.a.	4000	2500	2.5	n.a.	n.a.

Table A.3
Visco-elastic subsurface properties used in test 2 to simulate a shallow bedrock scenario.

Layer	*H* (m)	V_p (m/s)	V_s (m/s)	Rho (g/cm^3)	Q_p	Q_s
1	2.7778	330.2	206.4		30	15
2	2.7778	409.2	255.7	1.8	30	15
3	2.7778	461.2	288.2	1.8	30	15
4	2.7778	500	313.3	1.8	30	15
5	2.7778	1500	334.0	1.8	30	15
6	2.7778	1500	351.8	1.8	30	15
7	2.7778	1500	367.6	1.8	30	15
8	2.7778	1500	381.8	1.8	30	15
9	2.7778	1500	394.7	1.8	30	15
10	2.7778	1500	406.6	1.8	30	15
11	2.7778	1500	417.7	1.8	30	15
12	2.7778	1500	428.0	1.8	30	15
13	2.7778	1500	437.8	1.8	30	15
14	2.7778	1500	447.0	1.8	30	15
15	2.7778	1500	455.7	1.8	30	15
16	2.7778	1500	464.0	1.8	30	15
17	2.7778	1500	472.0	1.8	30	15
18	2.7778	1500	479.6	1.8	30	15
h.s.	n.a.	4000	2500	2.5	n.a.	n.a.

Appendix B. Summary of the results

Table B.1
Summary of the results obtained in this study.

	Subsurface perturbation	Simulation routine	F_0 deviance (%)	Average V_s deviance (%)	*H* deviance (%)
Test 1*	Normally dispersive	BW	<30% ↑	0	<25% ↓
		SW	<30% ↑	0	<25% ↓
	Inversely dispersive	BW	<35% ↓	0	<55% ↑
		SW	35%–55% ↓	0	60%–90% ↑
Test 2	Shallow ↑	BW		<10% ↑	<5% ↓
$H = 50$ m		SW			<5% ↓
	Middle ↑	BW		<8% ↑	<12% ↓
		SW			<12% ↓
	Deep ↑	BW		<8% ↑	<17% ↓
		SW			<17% ↓
	Shallow ↓	BW		<20% ↓	<10% ↑
		SW			<15% ↑
	Middle ↓	BW		<15% ↓	<30% ↑
		SW			<30% ↑
	Deep ↓	BW		<12% ↓	<40% ↑
		SW			<40% ↑
Test 2	Shallow ↑	BW		<12% ↑	<3% ↓
$H = 750$ m		SW			<7% ↓
	Middle ↑	BW		<8% ↑	<12% ↓
		SW			<12% ↓
	Deep ↑	BW		<5% ↑	<12% ↓
		SW			<14% ↓
	Shallow ↓	BW		<15% ↓	<5% ↑
		SW			<10% ↑
	Middle ↓	BW		<12% ↓	<20% ↑
		SW			<30% ↑
	Deep ↓	BW		<10% ↓	<30% ↑
		SW			<40% ↑

↑ increase/overestimation.
↓ decrease/underestimation.
BW: body waves-based modeling.
SW: surface waves-based modeling.
* Average V_s was kept constant.

Table B.2
The table summarizes the ranges of experimental uncertainty of bedrock depth evaluation available in literature as compared with depths of the corresponding test sites. It is introduced to the reader only for comparison purposes with the present study. As such it is not meant to represent a complete review of the literature on the topic.

Author	Maximum depth (m)	*H* error (%)	Test site
Ibs-von Seht and Wohlenberg (1999)	1250	<15 ÷ 20	Lower Rhine Embayment (Germany)
Delgado et al. (2000)	44	<15	Bajo Segura Basin (Spain)
Parolai et al. (2002)	1000	≤30[a] (underestimation)	Cologne (Germany)
D'Amico et al. (2004)	20 ÷ 24	20 ÷ 25	Le Piane basin (Italy)
Motamed et al. (2007)	80	4 ÷ 30	Bam area (Iran)
Guéguen et al. (2007)	>900	10 >50[b]	Grenoble Valley (France)
Gosar and Lenart (2010)	200	<20	Ljubljana Moor Basin (Slovenia)
Johnson and Lane (2016)	60	≤13	

[a] Using Ibs-von Seht and Wohlenberg (1999) relation. Better results were obtained with an ad-hoc calibration function.
[b] Local anomalous error, attributed to three-dimensional effects.

References

Abu Zeid, N., Bignardi, S., Caputo, R., Mantovani, A., Tarabusi, G., Santarato, G., 2014. Shear-wave velocity profiles across the Ferrara arc: a contribution for assessing the recent activity of blind tectonic structures. Proceedings of the 33th GNGTS National Convention. 1, pp. 117–122.

Abu Zeid, N., Corradini, E., Bignardi, S., Santarato, G., 2016. Unusual geophysical techniques in archaeology - HVSR and induced polarization, a case history. Proceedings of the NSAG-2016, 22nd European Meeting of Environmental and Engineering Geophysics. http://dx.doi.org/10.3997/2214-4609.201602027.

Abu Zeid, N., Corradini, E., Bignardi, S., Nizzo, V., Santarato, G., 2017. The Passive Seismic Technique 'HVSR' as a Reconnaissance Tool for Mapping Paleo-soils: The Case of the Pilastri Archaeological Site, Northern Italy, Archaeological Prospection. http://dx.doi.org/10.1002/arp.1568.

Bard, P.Y., 1998. Microtremor measurement: a tool for site effect estimation? Proceedings the Effects of Surface Geology on Seismic Motion, Yokohama Japan 3 1251–1279. Two-dimensional Seismic Wave Modeling and Inversion by the Boundary Element Method

Bignardi, S., Abu Zeid, N., Santarato, G., 2014. Thickness variations in layered subsurface models-effects on simulated MASW. Proceedings of the 76th EAGE Conference and Exhibition 2014; Amsterdam; Netherlands. http://dx.doi.org/10.3997/2214-4609.20140540.

Bignardi, S., Mantovani, A., Abu Zeid, N., 2016. OpenHVSR: imaging the subsurface 2D/3D elastic properties through multiple HVSR modeling and inversion. Comput. Geosci. 93 (1):103–113. http://dx.doi.org/10.1016/j.cageo.2016.05.009.

Bonnefoy-Claudet, S., Cornou, C., Bard, P.Y., Cotton, F., Moczo, P., Kristek, J., Donat, F., 2006. H/V ratio: a tool for site effects evaluation. Results from 1-D noise simulations. Geophys. J. Int. 167 (2):827–837. http://dx.doi.org/10.1111/j.1365-246X.2006.03154.x.

Cercato, M., 2015. Sensitivity analysis of Rayleigh-wave ellipticity with application to near surface characterization. Proceedings of the 21st European Meeting of Environmental and Engineering Geophysics, Near Surface Geoscience 2015. http://dx.doi.org/10.3997/2214-4609.201413713.

D13.08, 2004. Nature of Wave Field. Deliverable of the SESAME European Project, 50 Pages (Available on the SESAME website: http://SESAME-FP5.obs.ujf-grenoble.fr.).

D23.12, 2005. Guidelines for the Implementation of the H/V Spectral Ratio Technique on Ambient Vibrations Measurements, Processing and Interpretation, Deliverable of the SESAME European Project, 62 pages, April 2005. (Available on the SESAME web site: http://SESAME-FP5.obs.ujf-grenoble.fr.).

D'Amico, V., Picozzi, M., Albarello, D., Naso, G., Tropenscovino, S., 2004. Quick estimates of soft sediment thicknesses from ambient noise horizontal to vertical spectral ratios: a case study in southern Italy. J. Earthq. Eng. 8 (6):895–908. http://dx.doi.org/10.1142/S1363246904001729.

Delgado, J., Lo'pez Casado, C., Giner, J., Estévez, A., Cuenca, A., Molina, S., 2000. Microtremors as a geophysical exploration tool: applications and limitations. Pure Appl. Geophys. 157, 1445–1462.

Garcia-Jerez, A., Luzon, F., Navarro, M., Perez-Ruiz, A., 2006. Characterization of the sedimentary cover of the Zafarraya basin, southern Spain, by means of ambient noise. Bull. Seismol. Soc. Am. 96 (3):957–967. http://dx.doi.org/10.1785/0120050061.

Gosar, A., Lenart, A., 2010. Mapping the thickness of sediments in the Ljubljana Moor basin (Slovenia) using microtremors. Bull. Earthq. Eng. 8:501–518. http://dx.doi.org/10.1007/s10518-009-9115-8.

Guéguen, P., Cornou, C., Garambois, S., Banton, J., 2007. On the limitation of the H/V spectral ratio using seismic noise as an exploration tool: application to the Grenoble Valley (France), a small apex ratio basin. Pure Appl. Geophys. 164:115–134. http://dx.doi.org/10.1007/s00024-006-0151-x.

Herak, M., 2008. ModelHVSR - a Matlab tool to model horizontal-to-vertical spectral ratio of ambient noise. Comput. Geosci. 34, 1514–1526.

Hinzen, K.G., Scherbaum, F., Weber, B., 2004. On the resolution of H/V measurements to determine sediment thickness, a case study across a normal fault in the lower Rhine embayment, Germany. J. Earthq. Eng. 8 (6):909–926. http://dx.doi.org/10.1142/S136324690400178X.

Ibs-von Seht, M., Wohlenberg, J., 1999. Microtremor measurements used to map thickness of soft sediments. Bull. Seismol. Soc. Am. 89 (1), 250–259.

Johnson, C.D., Lane, J.W., 2016. Statistical comparison of methods for estimating sediment thickness from horizontal-to-vertical spectral ratio (HVSR) seismic methods: an example from Tylerville, Connecticut, USA. The 29th Annual Symposium on the Application of Geophysics to Engineering and Environmental Problems (SAGEEP), Denver, CO (March 20–24).

Lachet, C., Bard, P.Y., 1994. Numerical and theoretical investigations on the possibilities and limitations of Nakamura's technique. J. Phys. Earth 42, 377–397.

Lanzo, G., Silvestri, F., 1999. Risposta sismica locale. Teoria ed esperienze. Series: Argomenti di ingegneria geotecnica. Avelius editions (160 pp. EAN: 9788886977135 Book in Italian).

Lunedei, E., Albarello, D., 2010. Theoretical HVSR curves from full wavefield modelling of ambient vibrations in a weakly dissipative layered Earth. Geophys. J. Int. 181: 1093–1108. http://dx.doi.org/10.1111/j.1365-246X.2010.04560.x.

Motamed, R., Ghalandarzadeh, A., Tawhata, I., Tabatabaei, S.H., 2007. Seismic microzonation and damage assessment of Bam City, Southeastern Iran. J. Earthq. Eng. 11 (1), 110–132.

Mucciarelli, M., Gallipoli, M.R., 2001. A critical review of 10 years of Nakamura technique. Boll. Geofis. Teor. Appl. 42, 255–256.

Nakamura, Y., 1989. A method for dynamic characteristics estimation of subsurface using microtremor on the ground surface. Quarterly Report of Railway Technical Research Institute 30, 25–33.

Nakamura, Y., 2000. Clear identification of fundamental idea of Nakamura's technique and its applications. Proceedings of the 12th World Conference on Earthquake Engineering (8 pp., New Zealand).

Parolai, S., Bormann, P., Milkereit, C., 2002. New relationship between V_s, thickness of sediments, and resonance frequency calculated by the H/V ratio of seismic noise for the Cologne area (Germany). Bull. Seismol. Soc. Am. 92 (6):2521–2527. http://dx.doi.org/10.1785/0120010248.

Tsai, N.C., 1970. A note on the steady-state response of an elastic half-space. Bull. Seismol. Soc. Am. 60, 795–808.

Tsai, N.C., Housner, G.W., 1970. Calculation of surface motions of a layered half-space. Bull. Seismol. Soc. Am. 60, 1625–1651.

Wilken, D., Wunderlich, T., Majchczack, B., Andersen, J., Rabbel, W., 2015. Rayleigh-wave resonance analysis: a methodological test on a Viking age pit house. J. Cult. Herit. 9: 357–366. http://dx.doi.org/10.1002/arp.1508.